# AUXILIARY MEDIA – A GENERALIZED VIEW ON STACKING

*B. Schwarz, C. Vanelle, and D. Gajewski*

**email:** *benjamin.schwarz@zmaw.de*
**keywords:** *time imaging, stacking, auxiliary media*

## ABSTRACT

*Current multi-parameter stacking techniques aim to include higher order terms in the traveltime moveout surface. Without increasing the number of parameters, this goal is commonly achieved by assuming a certain reflector geometry and straight raypaths. In the presence of heterogeneity, as a consequence, moveout is described in an auxiliary medium. Although modern methods are usually based on the same set of parameters, we show that they can be divided into two types of approximations, one assuming an effective medium, the other describing the optical analogue in a medium of constant near-surface velocity. Based on ideas of de Bazelaire and Höcht et al., we present optical representations of effective medium operators currently in use. In addition, we clarify the unique role of the multifocusing method, theoretically and with synthetic examples, and point out distinct advantages of both approaches.*

## INTRODUCTION

Stacking still plays a fundamental role in seismic data processing. While the summation itself helps to decrease data redundancy and leads to a first interpretable time image with a high signal-to-noise ratio, the estimated parameters form the foundation of many important subsequent processing steps, including depth imaging.

In contrast to the classical NMO/DMO approach, recent works have indicated that even for complex settings, a macro-velocity model is not needed to perform all important time imaging tasks (e.g. Mann, 2002). Extending ideas of de Bazelaire (1988), the common reflection surface (CRS) stack takes neighbouring CMP gathers into account. It is based on three surface-related kinematic wavefield attributes, which are closely related to first- and second-order derivatives of the traveltime near the reference ray. In addition to the well-known parabolic and hyperbolic formulae (e.g. Jäger et al., 2001), several higher-order approximations exist, which all depend on the very same set of parameters.

In this work, we argue that without increasing the number of parameters, all higher-order approximations are based on the concept of straight rays, and consequently describe moveout in an auxiliary medium of constant velocity. Depending on the incorporation of parameters, the actual subsurface model is either replaced by a medium with effective properties or the method describes traveltime differences for the optical analogue in a medium of constant near-surface velocity.

Based on suggestions by de Bazelaire (1988) and Höcht et al. (1999), we establish a connection between both domains and provide a general recipe with which all effective medium operators can be transformed to their surface-based optical representations. Following this recipe, we introduce transformed versions of the hyperbolic CRS operator and the implicit CRS (i-CRS) approach by Vanelle et al. (2010) and Schwarz et al. (2012), which are both based on an effective medium.

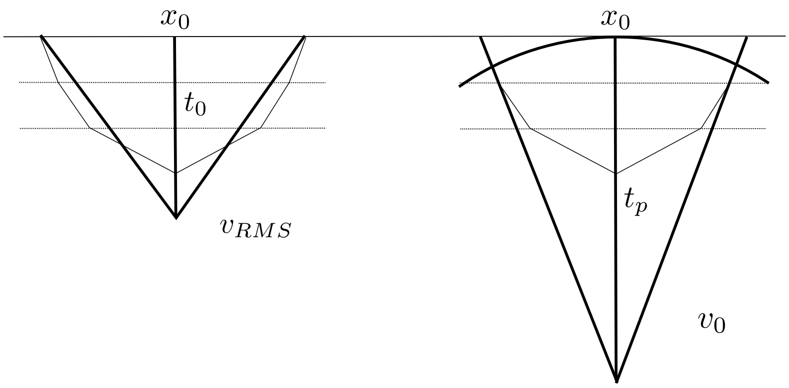


**Figure 1:** In the classical CMP stack, a vertically inhomogeneous model is replaced by an effective medium with the velocity $v_{RMS}$, denoting the root-mean-square velocity (left). The shifted hyperbola accounts for inhomogeneity by shifting the reference time $t_p$ (right).

The multifocusing method (MF, Gelchinsky et al., 1999) in contrast, being closely related to de Bazelaire's shifted hyperbola, has properties of an optical approach. Supporting these findings, both, multifocusing and the transformed i-CRS operator, turn out to perform equivalently for a simple synthetic example as well as the more complex Sigsbee 2a synthetic dataset. Concluding this paper, we shortly discuss distinct advantages of both concepts from a physical and an implementational point-of-view.

## AUXILIARY MEDIA

In the classical CMP stack (Mayne, 1962), the summation operator is a hyperbolic expression, which is only exact for a planar reflector and a constant velocity overburden. For the inhomogeneous case, the actual model is replaced by an effective medium with constant velocity. Thus, the NMO hyperbola is intrinsically based on the assumption of straight rays. De Bazelaire (1988) suggested an alternative strategy to account for heterogeneity by utilizing simple concepts of geometrical optics. In his approach (see Figure 1), not the velocity changes, but the centre of coordinates. Since this corresponds to the application of a shift in time rather than in velocity, de Bazelaire's shifted hyperbola, which depends only on the velocity near the surface, can be considered a macro-model independent time imaging method.

## OPTICAL REPRESENTATIONS

De Bazelaire's shifted reference $t_p$ (see below) is the zero-offset time in the optical image space of constant near-surface velocity $v_0$. It can be formulated in terms of the radius of curvature $R_{NIP}$ of the fundamental NIP wavefront (Hubral, 1983), which leads to an appealing geometrical interpretation (see Figure 2):

$$t_p = \frac{2R_{NIP}}{v_0} \quad . \tag{1}$$

Höcht et al. (1999) found that this interpretation not only holds for a layered medium, which was initially considered by de Bazelaire, but also for the general case of lateral inhomogeneity (compare Figure 2).

Due to coefficient comparisons, so-called osculating equations can be gained. These connect the effective to the surface-based attributes. Inspired by the work of Höcht et al. (1999), we suggest the following strategy to transform effective-medium-based traveltime operators to the optical image space:

1. Replace the actual zero-offset traveltime $t_0$ by its optical analogue (1),
2. Subtract the time shift $t_p - t_0$ from the total traveltime.

In the following section, we apply this strategy to the hyperbolic CRS operator and the recently introduced implicit CRS, and shortly elaborate on the role of the multifocusing approximation.

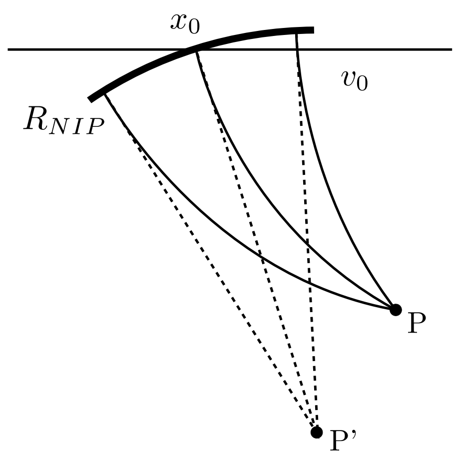


**Figure 2:** The optical methods approximate the moveout with the help of projections. A fictitious point source initiated at P in the actual model is assumed to produce the same measured wavefront as if the energy stemmed from point P' in a medium of constant near surface velocity $v_0$.

### Hyperbolic CRS

The CRS stack is an extension of the classical CMP stack, in which summation not only takes place in offset ($h$) but also in midpoint ($x_m$) direction. The hyperbolic CRS operator is closely related to the NMO hyperbola and thus describes traveltimes in an auxiliary medium of effective properties. According to Hertweck et al. (2007), it can be written as

$$t^2(\Delta x_m, h) = \left(t_0 + \frac{2\sin\alpha}{v_0}\Delta x_m\right)^2 + \frac{4\Delta x_m^2}{v_{CMO}^2} + \frac{4h^2}{v_{NMO}^2} \quad , \tag{2}$$

where $x_0$ is the horizontal position of the central midpoint and $v_{CMO}$ is a curvature dependent analogue of the NMO velocity. The connection of the two velocities to the surface-based kinematic wavefield attributes $\alpha$, $R_{NIP}$ and $R_N$ (Hubral, 1983) is established by the following set of osculating equations,

$$v_{NMO}^2 = \frac{2v_0 R_{NIP}}{t_0\cos^2\alpha} \quad , \tag{3a}$$

$$v_{CMO}^2 = \frac{2v_0 R_N}{t_0\cos^2\alpha} \quad . \tag{3b}$$

Like in the offset situation, the curvature-dependent velocity combines the wavefield attributes with the zero-offset traveltime. As a result, the CRS moveout also depends on $t_0$, which is characteristic for an effective-medium-based approach.

By the transformation according to the suggested recipe, we arrive at the optical representation of the CRS stack formula,

$$\left(t - t_0 + \frac{2R_{NIP}}{v_0}\right)^2 = \frac{4}{v_0^2}\left[(R_{NIP} + \sin\alpha\Delta x_m)^2 + \cos^2\alpha\left(\frac{R_{NIP}}{R_N}\Delta x_m^2 + h^2\right)\right] \quad , \tag{4}$$

which was also developed by Höcht et al. (1999). For horizontal layering ($\alpha = 0$) and vanishing midpoint displacement ($\Delta x_m = 0$), this shifted CRS equation reduces to de Bazelaire's shifted hyperbola. It is important to note that, like for the CMP setting, the moveout becomes independent of the zero-offset traveltime and is purely described by surface-related attributes.

### Implicit CRS

The i-CRS operator evaluates the reflection traveltime from a locally circular interface and is a pure double-square-root expression (Vanelle et al., 2010),

$$t(\Delta x_m, h) = t_s + t_g \quad , \tag{5}$$
$$t_s = \frac{1}{V}\sqrt{(\Delta x_m - h - \Delta x_c - R\sin\theta)^2 + (H - R\cos\theta)^2} \quad ,$$
$$t_g = \frac{1}{V}\sqrt{(\Delta x_m + h - \Delta x_c - R\sin\theta)^2 + (H - R\cos\theta)^2} \quad ,$$

where

$$\tan\theta = \frac{\Delta x_m - \Delta x_c}{H} + \frac{h}{H}\frac{t_s - t_g}{t_s + t_g} \quad , \tag{6}$$

and $\Delta x_c = x_c - x_0$. The link to the surface-related attributes is again established via a set of osculating equations, which, similar to (3) combine the wavefield attributes with the reference traveltime (Schwarz et al., 2012),

$$V = \frac{v_{NMO}}{\sqrt{1 + \frac{v_{NMO}^2}{v_0^2}\sin^2\alpha}} \quad , \tag{7a}$$
$$x_c = x_0 - \frac{R_N \sin\alpha}{\cos^2\alpha\left(1 + \frac{v_{NMO}^2}{v_0^2}\sin^2\alpha\right)} \quad , \tag{7b}$$
$$H = \frac{v_0 R_N}{v_{NMO}\cos^2\alpha\left(1 + \frac{v_{NMO}^2}{v_0^2}\sin^2\alpha\right)} \quad , \tag{7c}$$
$$R = \frac{\frac{v_0 R_N}{v_{NMO}\cos^2\alpha} - \frac{v_{NMO} t_0}{2}}{\sqrt{1 + \frac{v_{NMO}^2}{v_0^2}\sin^2\alpha}} \quad , \tag{7d}$$

with $v_{NMO}$ defined according to (3a). The traveltimes of the up- and downgoing ray segments are coupled via the angle $\theta$, which can be updated recursively following (6). The quantity $R$ represents the radius and $(x_c, H)$ denotes the position of the center of the circle approximating the reflector segment. Please note that $\Delta x_m - \Delta x_c = x_m - x_c$. While for a homogeneous overburden these parameters are directly linked to the subsurface geometry, they become effective properties for the heterogeneous case.

Following the transformation recipe, relations (7) simplify to

$$V = v_0 \quad , \tag{8a}$$
$$x_c = x_0 - R_N \sin\alpha \quad , \tag{8b}$$
$$H = R_N \cos\alpha \quad , \tag{8c}$$
$$R = R_N - R_{NIP} \quad , \tag{8d}$$

and the shifted i-CRS traveltime becomes

$$t - t_0 + \frac{2R_{NIP}}{v_0} = t_s(v_0, \alpha, R_{NIP}, R_N) + t_g(v_0, \alpha, R_{NIP}, R_N) \quad . \tag{9}$$

Like the shifted CRS moveout (see equation (4)), the shifted i-CRS moveout is independent of the zero-offset traveltime $t_0$ and entirely described in the auxiliary medium of constant near-surface velocity $v_0$.

### Multifocusing

Gelchinsky et al. (1999) introduced a double-square-root expression for the traveltime that depends on the same set of parameters as the CRS method, namely the kinematic wavefield attributes $\alpha$, $R_{NIP}$ and $R_N$.

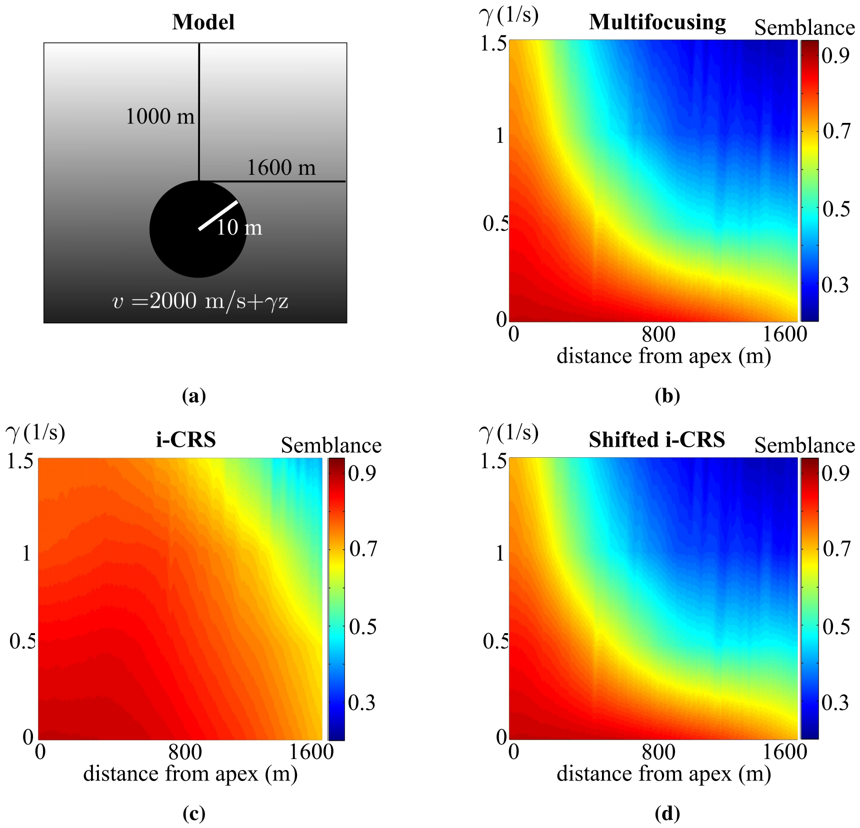


**Figure 3:** Underlying model (a) and corresponding semblance distributions for multifocusing (b), conventional i-CRS (c), and the shifted i-CRS expression (d).

Their operator describes the traveltime of a reflection event in terms of the traveltime of a central ray and corrections applied at source and receiver for a paraxial ray,

$$t(\Delta x_s, \Delta x_g) = t_0 + \Delta t_s + \Delta t_g \quad , \tag{10a}$$

$$\Delta t_s = \frac{\sqrt{R_s^2 + 2R_s \Delta x_s \sin\alpha + \Delta x_s^2} - R_s}{v_0} \quad , \tag{10b}$$

$$\Delta t_g = \frac{\sqrt{R_g^2 + 2R_g \Delta x_g \sin\alpha + \Delta x_g^2} - R_g}{v_0} \quad , \tag{10c}$$

where the radii $R_s$ and $R_g$ are functions of the CRS attributes (for details see, e.g., Landa et al., 2010). Please note that these two radii and, consequently, the multifocusing moveout does not depend on the zero-offset traveltime. In addition, (10a) can be rewitten in a time shift notation,

$$t - t_0 + \frac{R_s + R_g}{v_0} = t_s(v_0, \alpha, R_s) + t_g(v_0, \alpha, R_g) \quad ,$$

with $t_s = \Delta t_s + R_s/v_0$ and $t_g = \Delta t_g + R_g/v_0$. It reduces to de Bazelaire's shifted hyperbola for the CMP configuration, implying that it is natively based on concepts of geometrical optics.

## SYNTHETIC EXAMPLES

To get a better idea how the optical representations behave in an actual data application, we have investigated two synthetic examples of different complexity. The first example considers the diffraction

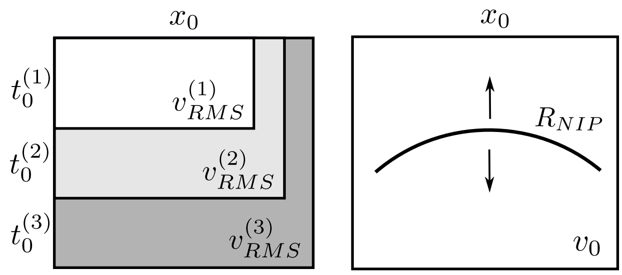


**Figure 4:** While effective media change their properties for each time sample due to their dependency on the reference time $t_0$ (left), the moveout for the optical methods is purely surface-related and may be precalculated in grid-based parameter searches (right).

case in a constant vertical velocity gradient medium $v = 2000$ m/s$+\gamma z$, with $\gamma$ ranging from 0 for the homogeneous case to 1.5 $s^{-1}$, representing strong vertical inhomogeneity. A sketch of the gradient model can be found in Figure 3(a).

Figure 3 shows the achieved semblance values of multifocusing and both, conventional i-CRS (expressions (5) with (7)) and its optical representation (equations (9) and (8)) as a function of the distance from the apex and the strength of the gradient. Multifocusing (Figure 3(b)) provides a good description for moderate and small gradients. However, it shows a rapidly decreasing performance for stronger gradients and larger distances to the apex. The conventional i-CRS operator, in turn, despite being parameterized with the same attributes and having the same double-square-root shape, turns out to be considerably less affected by heterogeneity. The shifted version of the i-CRS approximation reveals exactly the same semblance distribution as multifocusing, indicating that time-shift-based parameterizations are less suited to account for inhomogeneity than their effective medium counterparts (compare Figure 3(c) and 3(d)).

The same behaviour occurs for the more complex Sigsbee 2a synthetic dataset. In Figure 5, the semblance deviations between both i-CRS operators and multifocusing are displayed. While the differences are noticeable for conventional i-CRS, they mostly vanish for the shifted approach. Observe in Figure 6 that the conceptual connection of shifted i-CRS and multifocusing also shows in the estimation of the attributes.

## PRACTICAL CONSIDERATIONS

The synthetic examples indicate that the auxiliary medium underlying the parameterization of a stacking operator has an impact on its performance for stronger overburden heterogeneity. Since the zero-offset traveltime is used as input in the stacking procedure, it serves as a direct link to the data und thus to the actual subsurface model. The effective medium parameters in that sense are linked to the model, since they all have in common that $t_0$ is combined with the surface-related attributes in the osculating equations. As a result, the traveltime moveout always depends on $t_0$ for these operators, resulting in wavelet stretch during moveout correction.

The optical methods on the other hand reveal a high potential for efficient implementation (see Figure 4). Since moveout is always independent of the zero-offset traveltime, grid-based parameter searches can be accelerated by precalculating all possible moveouts outside of the time loop. While the effective medium parameters change for each time sample, the optical representations describe the moveout always in the same medium of constant $v_0$.

## CONCLUSIONS

We found that current multiparameter stacking techniques can be divided into two groups of approximations, one assuming an effective medium, the other dealing with projections in the optical image space.

While the hyperbolic CRS operator is closely related to the NMO hyperbola, which substitutes the actual subsurface model by a medium of a constant effective velocity, the multifocusing method reveals a strong link to the shifted hyperbola by de Bazelaire, which is an optical approach. The implicit CRS, like hyperbolic CRS, is an effective medium operator. Based on ideas of de Bazelaire and Höcht et al., we have presented a general recipe that allows for a simple transformation from the effective medium to optical image space. Applied to CRS and i-CRS we introduced time-shifted versions, i.e. optical representations of both operators. Synthetic examples reveal that the effective-medium-based conventional i-CRS operator is only mildly affected by overburden heterogeneity, whereas the shifted counterpart shows considerably decreased quality for higher gradients. Multifocusing, being a native optical image space approach, showes the exact same behaviour for the considered gradient example, as well as for the complex Sigsbee 2a dataset. Since moveout in image space is independent of the zero-offset traveltime, the optical methods are less suited to account for strong inhomogeneity but promise a high potential for efficient implementation, because moveouts can be precalculated in grid-based parameter searches.

## ACKNOWLEDGEMENTS

We thank the Applied Seismics Group Hamburg for continuous discussions. The Sigsbee 2a synthetic data were produced by the Subsalt Multiples Attenuation and Reduction Technology Joint Venture (SMAART JV). This work was partly supported by the sponsors of the Wave Inversion Technology (WIT) Consortium and the project 'Imaging steep structures with diffractions' (BMU 0325363C).

## REFERENCES

de Bazelaire, E. (1988). Normal moveout revisited – inhomogeneous media and curved interfaces. *Geophysics*, 53:143–157, doi:10.1190/1.1442449.

Gelchinsky, B., Berkovitch, A., and Keydar, S. (1999). Multifocusing homeomorphic imaging – part 1. Basic concepts and formulae. *Journal of Applied Geophysics*, 42:229–242, doi:10.1016/S0926–9851(99)00038–5.

Hertweck, T., Schleicher, J., and Mann, J. (2007). Data stacking beyond CMP. *The Leading Edge*, 26(7):818–827, doi:10.1190/1.2756859.

Höcht, G., de Bazelaire, E., Majer, P., and Hubral, P. (1999). Seismics and optics: hyperbolae and curvatures. *Journal of Applied Geophysics*, 42:261–281, doi:10.1016/S0926–9851(99)00040–3.

Hubral, P. (1983). Computing true amplitude reflections in a laterally inhomogeneous earth. *Geophysics*, 48:1051–1062, doi:10.1190/1.1441528.

Jäger, R., Mann, J., Höcht, G., and Hubral, P. (2001). Common-reflection-surface stack: Image and attributes. *Geophysics*, 66:97–109, doi:10.1190/1.1444927.

Landa, E., Keydar, S., and Moser, T. J. (2010). Multifocusing revisited – inhomogeneous media and curved interfaces. *Geophysical Prospecting*, 58:925–938, doi:10.1111/j.1365–2478.2010.00865.x.

Mann, J. (2002). *Extensions and Applications of the Common-Reflection-Surface Stack Method*. PhD thesis, Universität Karlsruhe.

Mayne, W. H. (1962). Common reflection point horizontal data stacking techniques. *Geophysics*, 27:927–938, doi:10.1190/1.1439118.

Schwarz, B., Vanelle, C., Kashtan, B., and Gajewski, D. (2012). i–CRS: application of a new multiparameter stacking approach to complex media. *SEG, Expanded Abstracts*, pages doi:10.1190/segam2012–1542.1.

Vanelle, C., Kashtan, B., Dell, S., and Gajewski, D. (2010). A new stacking operator for curved subsurface structures. *SEG, Expanded Abstracts*, 29:3609–3613, doi:10.1190/1.3513600.

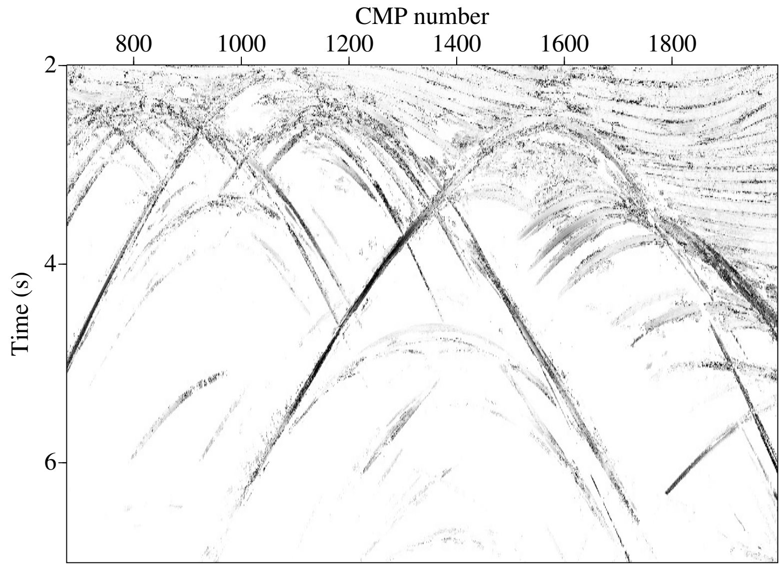


**(a)**

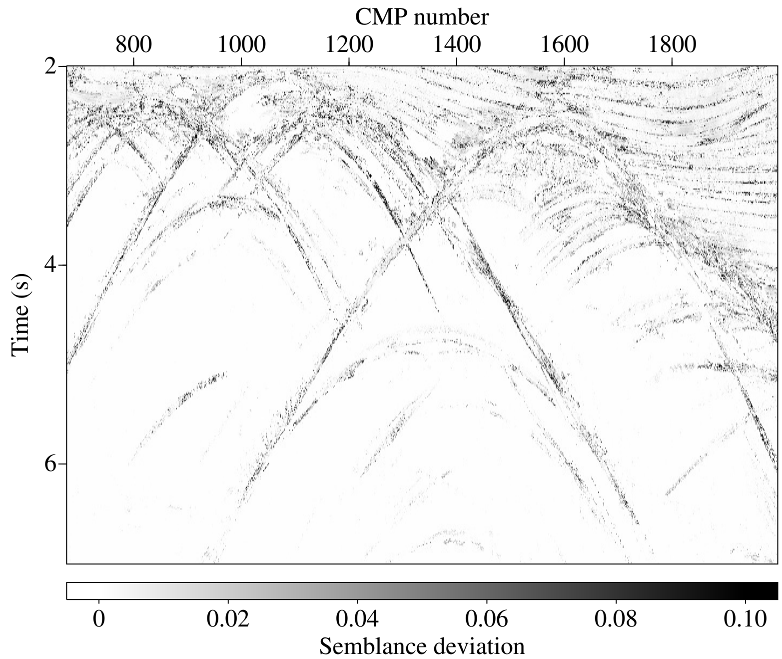


**(b)**

**Figure 5:** Difference in semblance for a part of the Sigsbee 2a model. Multifocusing is compared (a) with conventional i-CRS and (b) with the shifted i-CRS operator. Conventional i-CRS, being an effective medium formula, shows higher semblance values than the optical methods for medium to large distances to the diffraction apices.

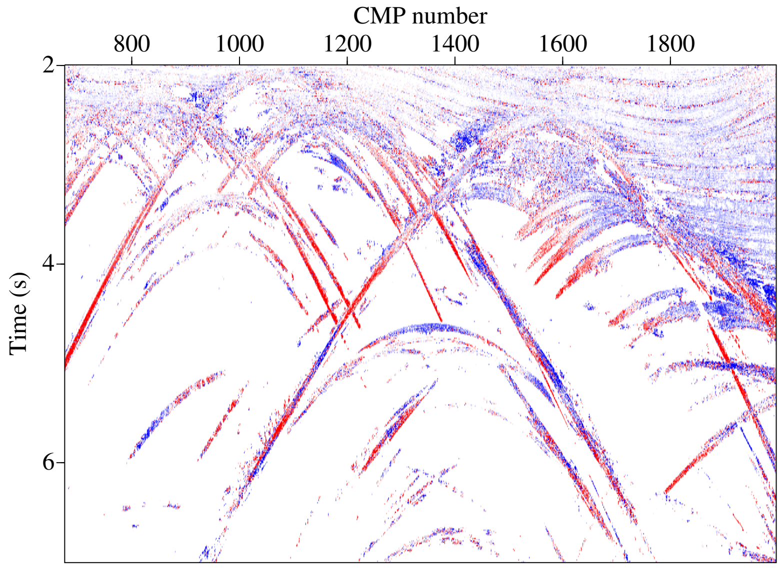


**(a)**

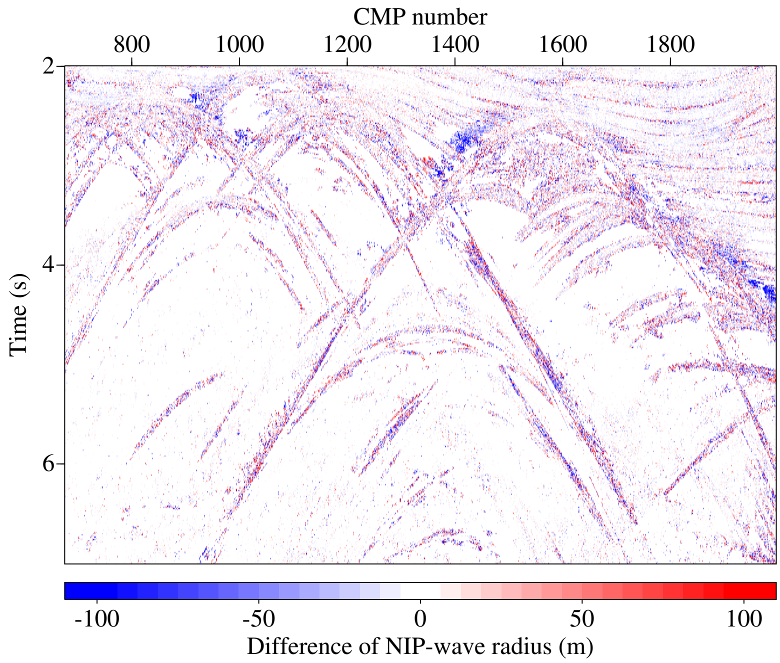


**(b)**

**Figure 6:** Difference in $R_{NIP}$ for a part of the Sigsbee 2a model. Multifocusing is compared (a) with conventional i-CRS and (b) with the shifted i-CRS operator and serves as the reference. While shifted i-CRS and multifocusing provide similar estimates throughout the section, i-CRS differs noticeably.